

Image Segmentation with Thresholding based on Relative Arithmetic-Geometric Divergence

Fangyan Nie, *Member, IAENG*, and Jianqi Li

Abstract—Image segmentation by thresholding has been widely used in industrial practice. Due to the complexity of the real environment, the universality of image segmentation algorithm is greatly challenged, so different segmentation methods need to be designed for different application scenarios. In information theory, the relative arithmetic-geometric divergence is an efficient information distance measure used to measure similarity (or dissimilarity) between different information systems. It overcomes the deficiency of traditional divergence measure and can better reflect the similarity or dissimilarity between different systems. In this paper, an image threshold segmentation method is designed and implemented based on relative arithmetic-geometric divergence. The presented method is applied to the segmentation of nondestructive testing images, degraded document images, medical images and security inspection surveillance images. In comparison with some classical image threshold segmentation algorithms, the effectiveness of the proposed method is verified successfully. For the proposed method, it provides the advantages of briefer algorithm, easy to implement, and less computing time. The proposed method can meet with the real time requirement, and it has a good prospect of application and far-reaching research value.

Index Terms—image segmentation, thresholding, information distance, divergence measure, arithmetic-geometric.

I. INTRODUCTION

IMAGE segmentation is one of the most basic, but also the most difficult and challenging problems in image processing [1], [2]. The purpose of image segmentation is to divide the image into multiple non-overlapping regions with similar content or characteristics, and lays the foundation for the subsequent processing. Because of various factors in image imaging, image is a complex information system. Any segmentation method can not be applied to all images. Therefore, engineers or researchers need to design appropriate methods according to specific segmentation task requirements. Thus, various image segmentation methods are constantly emerging [3], [4].

The method based on the concept of entropy in information theory (such as Shannon entropy, cross entropy, etc.) is one of the most widely used thresholding method in image thresholding technology [5]–[12]. Entropy-based thresholding methods have a solid physics theory as a basis and high efficiency in image segmentation, so it has been extremely favored by researchers and engineers. Therefore,

Manuscript received February 2, 2022; revised May 20, 2022. This work was supported in part by the Research Foundation of Department of Education of Hunan Province, China (Grant No.18A368) and the Natural Science Foundation of Hunan Province, China (Grant No.2021JJ50022, 2021JJ30477).

Fangyan Nie is a Professor of College of Computer and Electrical Engineering, Hunan University of Arts and Science, Hunan, 415000 China (phone: +86-736-7187895, e-mail: niefyan@huas.edu.cn).

Jianqi Li is a Professor of Hunan Provincial Key Laboratory of Distributed Electric Propulsion Vehicle Control Technology, Hunan, 415000 China (e-mail: li_jianqi@126.com).

methods or improvement schemes based on the concept of entropy have emerged in research or application. Among them, the method based on cross entropy is one of the most widely used entropy threshold segmentation method in practice [8]–[12]. This method was originally proposed by Li and Lee [8]. Cross entropy, also known as information divergence or relative entropy, is a measure used to measure the difference or information distance between different information systems. In image thresholding, cross entropy is used as a tool to measure the loss of information between segmented image and original image. The smaller the cross entropy between segmented image and original image, the higher the quality of the segmented image. The minimum cross entropy thresholding method proposed by Li and Lee [8] is the most famous image threshold segmentation method based on cross entropy. Another famous thresholding methods related to the concept of cross entropy is the minimum error thresholding method proposed by Kittler and Illingworth [13]. This method is essentially a relative entropy method based on the concept of mean square error of Euclidean distance [14], [15]. The mean square error cannot completely and effectively distinguish the relationship between image pixels, so it also has some shortcomings in image segmentation [16].

Relative arithmetic-geometric divergence is an efficient information distance measure proposed by Taneja [17], on the basis of analyzing the traditional information divergence (cross entropy) measure to measure the similarity (or dissimilarity) between different information systems. This measure overcomes the shortcomings of the traditional divergence measure and can better reflect the similarity or dissimilarity between different systems. Image is a complex information system, and the distribution of pixels information varies greatly according to the imaging mode and process. Therefore, in the process of segmentation, the measurement method of information difference between image pixels also seriously affects the segmentation performance. Based on arithmetic-geometric divergence, this paper proposes a thresholding method to improve the performance of image segmentation.

Nondestructive testing image segmentation [18], [19], medical image segmentation and security inspection surveillance images segmentation are widely used in real life or practical production. In order to verify the effectiveness of the proposed method, based on the comparison with some classical image threshold segmentation methods (such as maximum between-cluster variance method [20], minimum cross entropy method [8], minimum error thresholding method [13], etc.), comprehensive experiments are carried out on the above images. The experimental results show that the proposed method has good segmentation performance, is easy to implement, and has great application value and good

popularization prospect.

II. METHODOLOGY OF PROPOSED METHOD

A. Relative Arithmetic-Geometric Divergence

Let $\Omega_n = \{P = (p_1, p_2, \dots, p_n) | p_i > 0, \sum_{i=1}^n p_i = 1\}$, $n \geq 2$, be the set of complete finite discrete probability distribution. Let $P, Q \in \Omega_n$, the relative arithmetic-geometric divergence [17] is defined as follows.

$$D(P|Q) = \sum_{i=1}^n \left[\left(\frac{p_i + q_i}{2} \right) \log \left(\frac{p_i + q_i}{2p_i} \right) \right] \quad (1)$$

Where P and Q represent two discrete finite probability distributions, and $D(P|Q)$ is used to measure the information difference between P and Q . The smaller the value of $D(P|Q)$, the more similar the probability distributions P and Q .

B. The Proposed Method

The basic idea of image threshold segmentation using arithmetic-geometric divergence is as follows.

Firstly, input the image to be segmented and calculate its normalized grayscale histogram. Then, construct the relative arithmetic-geometric divergence between segmented image and original image. Thirdly, search the grayscale that makes the divergence obtain minimum value within the grayscale range of image. Finally, use the obtained grayscale to perform thresholding and output the segmented image.

To sum up, the steps of applying relative arithmetic-geometric divergence to image threshold segmentation are described as follows.

Step 1: Read the gray image with size of $m \times n$ to be segmented, and store it in a two-dimensional image array I .

Step 2: Construct grayscales set $G = \{0, 1, \dots, L-1\}$; Calculate the normalized grayscale histogram H ($H = \{h_0, h_1, \dots, h_{L-1}\}$) of image I through formula $h_i = n_i / (m \times n)$, where n_i represents the number of pixels with gray level i in image I , $L-1$ represents the maximum gray level in image I , and $L = 256$ for 8-bit digital image.

Step 3: Assume that t is a segmentation threshold, then t divides image pixels into two gray level sets of different classes, i.e., C_0 and C_1 , where $C_0 = \{0, 1, 2, \dots, t\}$, $C_1 = \{t+1, t+2, \dots, L-1\}$.

Step 4: Take H as the probability density function estimation of image grayscales, and then a prior probabilities P_0 and P_1 about C_0 and C_1 can be calculated as follows.

$$P_0 = \sum_{i=0}^t h_i, \quad P_1 = \sum_{i=t+1}^{L-1} h_i \quad (2)$$

Step 5: Calculate the grayscale mean m_0 and m_1 about C_0 and C_1 based on Equation (3).

$$m_0 = \sum_{i=0}^t i \cdot h_i / P_0, \quad m_1 = \sum_{i=t+1}^{L-1} i \cdot h_i / P_1 \quad (3)$$

Step 6: Calculate the relative arithmetic-geometric divergence D_0 and D_1 about C_0 and C_1 according to Equations (4) and (5).

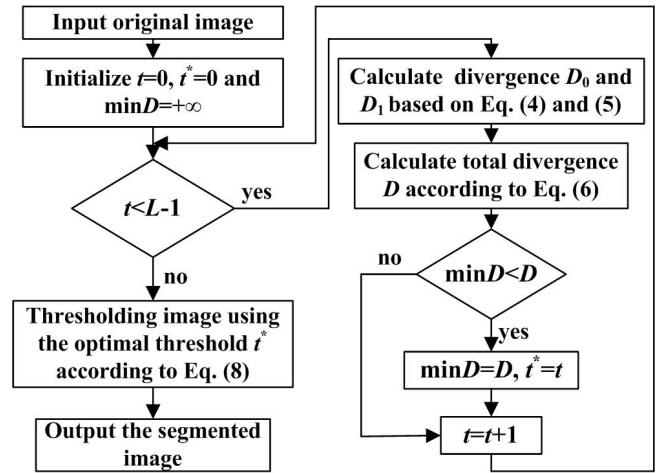


Fig. 1. Algorithm flow chart of the proposed method

$$D_0 = \sum_{i=0}^t \left\{ h_i \left[\left(\frac{i + m_0}{2} \right) \log \left(\frac{i + m_0}{2 \times i} \right) \right] \right\} \quad (4)$$

$$D_1 = \sum_{i=t+1}^{L-1} \left\{ h_i \left[\left(\frac{i + m_1}{2} \right) \log \left(\frac{i + m_1}{2 \times i} \right) \right] \right\} \quad (5)$$

Step 7: Construct the criterion function for image threshold segmentation through Equations (4) and (5), as shown in Equation (6).

$$D = D_0 + D_1 \quad (6)$$

Step 8: In the range of $G = \{0, 1, \dots, L-1\}$, search the grayscale t^* using Equation (7) that makes Equation (6) obtain the minimum value, that is, t^* is the optimal segmentation threshold.

$$t^* = \arg \min_{t \in G} [D] \quad (7)$$

Step 9: Assuming that $f(x, y)$ represents the pixel gray value at the image coordinate (x, y) of the original image I and $s(x, y)$ represents the pixel gray value at the image coordinate (x, y) of segmented image S , $s(x, y)$ can be calculated by Equation (8) after obtaining the optimal segmentation threshold t^* .

$$s(x, y) = \begin{cases} 0, & \text{if } (f(x, y) \leq t^*) \\ L-1, & \text{if } (f(x, y) > t^*) \end{cases} \quad (8)$$

Step 10: Output the segmented image S .

C. Algorithm Flow diagram

The algorithm flow diagram of the proposed method is shown in Figure 1.

III. EXPERIMENTS AND ANALYSIS

In order to illustrate the effectiveness of the method proposed in this paper, we compared the performance of the proposed method with some classical image thresholding methods, such as the maximum between-cluster variance method proposed by Otsu (which is also widely known as Otsu method in research literature) [20], the minimum error

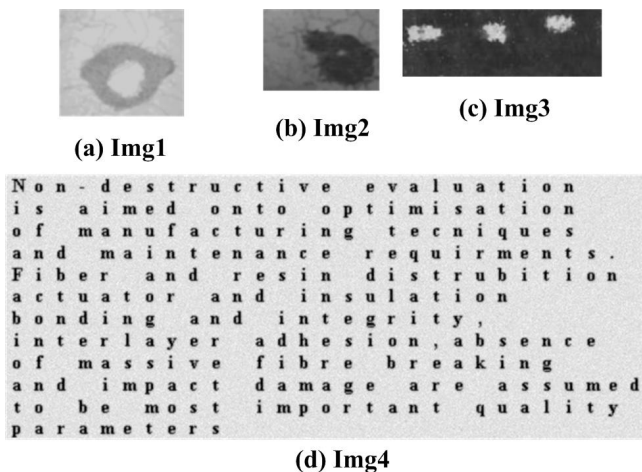


Fig. 2. The tested images for performance evaluation

thresholding method proposed by Kittler and Illingworth [13], and the minimum cross entropy thresholding method proposed by Li and Lee [8]. In addition, an improved Tsallis entropy method proposed by Lin and Ou [21], and an improved Otsu method proposed by Cai et al. [19] are also compared with the proposed method. For the convenience of description, in the following, we refer to the above methods as Otsu method, MET method, MCE method, Lin method, Cai method and proposed method, respectively.

During the experiment, the configuration of experimental environment is as follows: A laptop computer with Intel(R) Core (TM) i7-8550U CPU @1.80GHz 1.99 GHz, 16.0GB memory, and 64-bit Windows 11 Home China operating system. The methods used to performance comparison are implemented by 64-bit MATLAB R2010a programming language.

A. Performance Evaluation

The Otsu method has a prominent position in the field of image thresholding [10], [12], [18]–[20], [22]. The MET method is a thresholding method that closely related to the concept of relative entropy (i.e. cross entropy) [15]. The MCE method is the most famous cross entropy method [8]–[11]. Lin method has been successfully applied in practice as a method related to the concept of entropy [21], and Cai method [19] has been successfully applied on nondestructive testing images as an improved Otsu method. Therefore, the above methods are compared with the proposed method in this paper.

In this subsection, the images for performance evaluation are selected from reference [18]. There are both original images, and the corresponding ground-truths that manually segmented by experts for the images provided by [18]. These images are very convenient for objective evaluation of image segmentation method performance, and have been widely used in many literature [18].

Here, three nondestructive testing images and one degraded document image are selected for performance evaluation. These four original images are shown in Figure 2. For the convenience of description, we call these four images as ‘Img1’, ‘Img2’, ‘Img3’, and ‘Img4’, respectively.

In Figure 2, ‘Img1’ is a defective eddy current image, ‘Img2’ and ‘Img3’ are two material images. These three

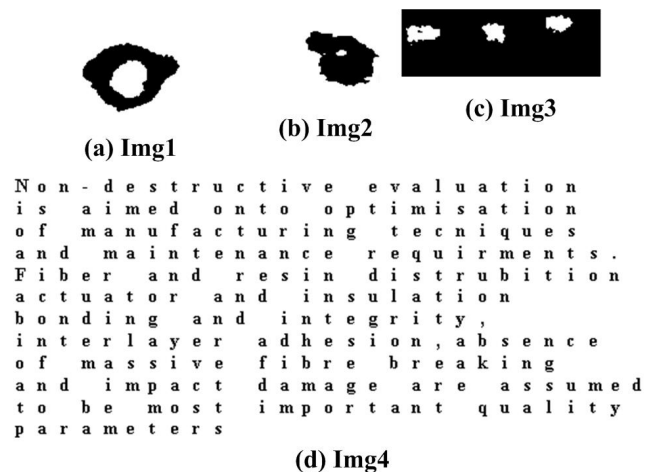


Fig. 3. The ground-truths of tested images

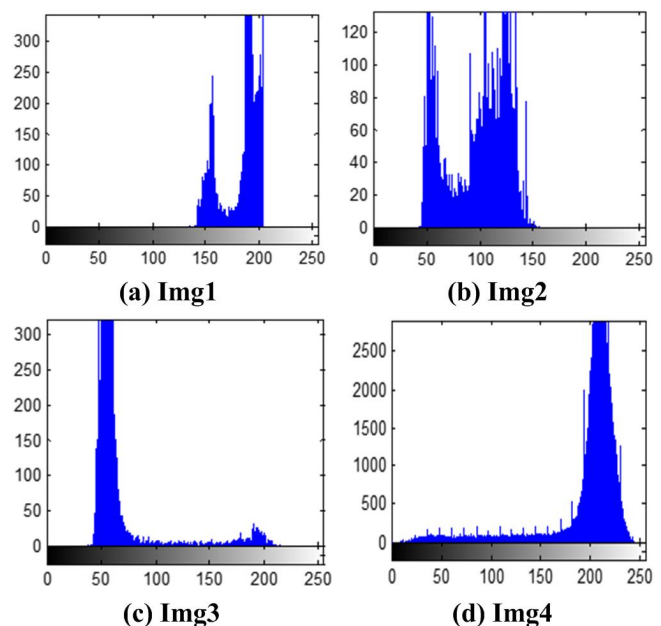


Fig. 4. The histograms of four tested images

images are nondestructive testing images. ‘Img4’ is a degraded document image. For these four images, their sizes are 92×107 , 70×100 , 58×171 , and 227×551 , respectively.

The corresponding ground-truths of the above four images are shown in Figure 3. The grayscale histograms of the four images are shown in Figure 4.

As can be seen from Figure 2, for the four images used for performance evaluation, the area of object of each image accounts for a small proportion of the whole image area, which can also be seen from Figure 4. In Figure 4, the grayscale histogram distribution of each image presents a complex unimodal or bimodal distribution. For image object of each image, its grayscale distribution is not in the dense area of the grayscale distribution of the whole histogram, and the proportion is relatively small. Therefore, there is a certain difficulty in segmentation for these images.

Figure 5 shows the segmentation results of ‘Img1’. It can be seen from Figure 5 that the object is basically not separated for the result obtained by MET method, and there are too many noise pixels in the result obtained by Lin method. The objects are separated well for the results

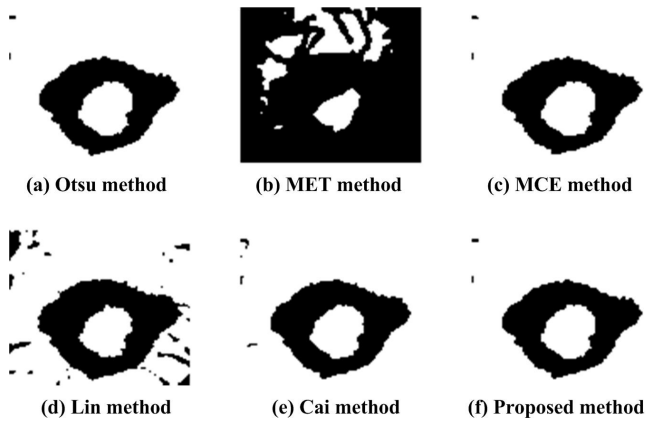


Fig. 5. The threshold segmentation results of Img1

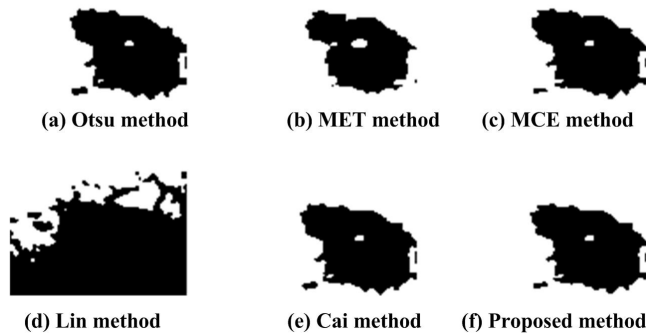


Fig. 6. The threshold segmentation results of Img2

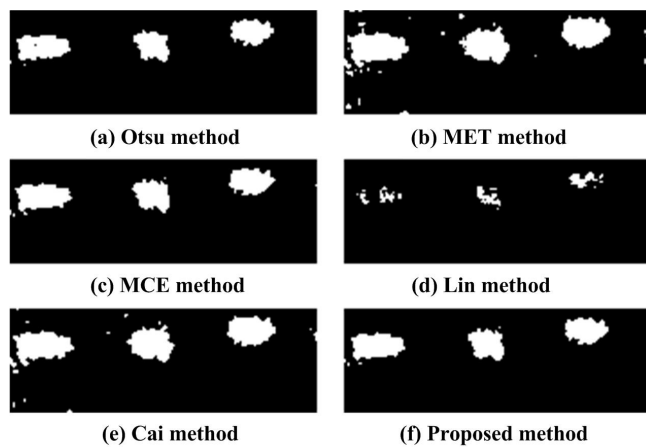


Fig. 7. The threshold segmentation results of Img3

obtained by other four methods, and these four results are far better than those obtained by MET and Lin methods.

Figure 6 shows the segmentation results of ‘Img2’. As can be seen from Figure 6, except for Lin method, other methods are better to separate the image object from the background.

Figure 7 shows the segmentation results of ‘Img3’. As can be seen from Figure 7, the object separated by Lin method is broken and incomplete. The results obtained by MET method and Cai method have some residual noise pixels. For other three methods, the object contour is complete and the edge is smooth in the results obtained by them.

Figure 8 shows the segmentation results of image ‘Img4’ by every method. As can be seen from Figure 8, the characters in the results obtained by MET method and

TABLE I
THE OPTIMAL THRESHOLDS OBTAINED BY 6 METHODS

Tested images	Img1	Img2	Img3	Img4
Otsu method	175	88	115	144
MET method	203	69	71	177
MCE method	174	84	101	128
Lin method	186	120	194	181
Cai method	178	87	76	167
Proposed method	175	85	109	124

Lin method are blurred, and the ‘words’ in the segmented images cannot be easily identified. The characters in the result obtained by Cai method is conglutination, and the ‘words’ in the segmented image cannot be discriminated well. However, the result obtained by Cai method is slightly better than those obtained by MET method and Lin method from visual analysis. The results obtained by Otsu method, MCE method and the proposed method are much better than those obtained by the other three methods. The results obtained by these three methods better “pull out” the ‘words’ from the background.

From Figures 5-8, we can see that, the Otsu method, the MCE method and the proposed method achieve better results on the segmentation of test images than other methods. The Otsu method and the MCE method are the two most famous image thresholding segmentation methods. Compared with them, the segmentation results obtained by the proposed method are not worse, which also proves the effectiveness of the proposed method from one aspect.

Table 1 lists the optimal thresholds obtained by 6 methods on the four tested images.

It can be seen from Table 1 and Figure 4 that the optimal thresholds obtained by proposed method are closer to the valley position of the image graylevel histogram. Generally speaking, if an image can be segmented by thresholding and get better results, the optimal threshold is located near the valley of the histogram. This also shows the effectiveness of the proposed method.

The above analysis is based on visual qualitative analysis. In order to more objectively illustrate the effectiveness of each method, some more objective criteria will be used to illustrate the performance of each method in the following.

Here we firstly define three parameters, namely *NTMP*, *NMOP*, and *NMBP*, and their meanings are as follows. *NTMP* represents the total number of misclassified pixels in the image; *NMOP* represents the number of object pixels in the image that are classified as background pixels; *NMBP* represents the number of background pixels in the image that are classified as object pixels. For *NTMP*, *NMOP* and *NMBP*, the smaller their values, the better the performance of the threshold segmentation method.

Tables 2-4 list the statistical results for these three parameters obtained by each method on four performance test images.

It can be seen from Table 3 that, no or very few image object pixels are incorrectly classified as background pixels except Lin method on ‘Img3’ image. Therefore, from *NMOP* indicator, the performance of each method is acceptable.

However, looking at Table 4, we can see that, there are too many background pixels to be incorrectly classified as

Non-destructive evaluation is aimed onto optimisation of manufacturing techniques and maintenance requirements. Fiber and resin distribution actuator and insulation bonding and integrity, interlayer adhesion, absence of massive fibre breaking and impact damage are assumed to be most important quality parameter

(a) Otsu method

Non-destructive evaluation is aimed onto optimisation of manufacturing techniques and maintenance requirements. Fiber and resin distribution actuator and insulation bonding and integrity, interlayer adhesion, absence of massive fibre breaking and impact damage are assumed to be most important quality parameters

(b) MET method

Non-destructive evaluation is aimed onto optimisation of manufacturing techniques and maintenance requirements. Fiber and resin distribution actuator and insulation bonding and integrity, interlayer adhesion, absence of massive fibre breaking and impact damage are assumed to be most important quality parameters

(c) MCE method

Non-destructive evaluation is aimed onto optimisation of manufacturing techniques and maintenance requirements. Fiber and resin distribution actuator and insulation bonding and integrity, interlayer adhesion, absence of massive fibre breaking and impact damage are assumed to be most important quality parameters

(d) Lin method

Non-destructive evaluation is aimed onto optimisation of manufacturing techniques and maintenance requirements. Fiber and resin distribution actuator and insulation bonding and integrity, interlayer adhesion, absence of massive fibre breaking and impact damage are assumed to be most important quality parameters

(e) Cai method

Non-destructive evaluation is aimed onto optimisation of manufacturing techniques and maintenance requirements. Fiber and resin distribution actuator and insulation bonding and integrity, interlayer adhesion, absence of massive fibre breaking and impact damage are assumed to be most important quality parameters

(f) Proposed method

Fig. 8. The threshold segmentation results of Img4

object pixels for MET method on 'Img1' and 'Img4' images, Lin method on 'Img2' and 'Img4' images, Cai method on 'Img4' image. For Otsu, MCE, and the proposed methods,

TABLE II
THE STATISTICAL RESULTS OF NTMP

Tested images	Img1	Img2	Img3	Img4
Otsu method	12	463	75	587
MET method	5835	29	501	9037
MCE method	40	364	155	107
Lin method	676	3071	542	7440
Cai method	100	440	389	3319
Proposed method	12	394	111	131

TABLE III
THE STATISTICAL RESULTS OF NMOP

Tested images	Img1	Img2	Img3	Img4
Otsu method	0	0	0	0
MET method	0	26	0	0
MCE method	29	0	0	21
Lin method	0	0	542	0
Cai method	0	0	0	0
Proposed method	0	0	0	13

TABLE IV
THE STATISTICAL RESULTS OF NMBP

Tested images	Img1	Img2	Img3	Img4
Otsu method	12	463	75	587
MET method	5835	3	501	9037
MCE method	11	364	155	86
Lin method	676	3071	0	7440
Cai method	100	440	389	3319
Proposed method	12	394	111	118

the background pixels, those to be incorrectly classified as object pixels are much less than MET, Lin, and Cai methods on these images. On all test images, the misclassified background pixels of the proposed method are similar to or less than those of Otsu and MCE methods.

Looking at Table 2 again, in comparison, the pixel classification results of the proposed method are slightly better than those of Otsu and MCE methods, but it is much better than the other three methods. The sum of the misclassified pixels on all images is 648 for the proposed method, it is smaller than that obtained by Otsu and MCE methods (1137 for Otsu method and 666 for MCE method). The results of Otsu method and MCE method are better than MET, Lin and Cai methods. The worst performer is MET method, followed by Lin method. In conjunction with Figures 5-8, these analyses are also consistent with the visual observations.

In addition, we further use the misclassification error rate (MER) to describe the performance of each method. MER is a widely used performance evaluation index in the research of image segmentation [18]. The value range of MER is [0,1], the smaller the value, the better the performance of the segmentation algorithm. MER is defined as follows.

$$MER = \frac{NTMP}{Total\ number\ of\ pixels\ in\ image} \times 100\% \quad (9)$$

Table 5 lists the comparison of MER of every method on four test images. From Table 5, we can see that, the values of MER obtained by MET method on 'Img1' and 'Img4' images, Lin method on 'Img2' and 'Img4' images, and Cai

TABLE V
THE COMPARISON OF PIXEL MISCLASSIFICATION ERROR RATE

Tested images	Img1	Img2	Img3	Img4
Otsu method	0.0012	0.0661	0.0076	0.0047
MET method	0.5927	0.0041	0.0505	0.0723
MCE method	0.0041	0.0520	0.0156	0.0009
Lin method	0.0687	0.4387	0.0546	0.0595
Cai method	0.0102	0.0629	0.0392	0.0265
Proposed method	0.0012	0.0563	0.0112	0.0010

TABLE VI
THE COMPUTING TIME OF EACH METHOD ON TEST IMAGES (SECOND)

Tested images	Img1	Img2	Img3	Img4
Otsu method	0.0398	0.0381	0.0463	0.1216
MET method	0.0065	0.0086	0.0088	0.0158
MCE method	0.0076	0.0082	0.0100	0.0178
Lin method	0.0050	0.0065	0.0086	0.0173
Cai method	0.0087	0.0099	0.0138	0.0242
Proposed method	0.0076	0.0087	0.0104	0.0193

methods on ‘Img4’ image are significantly greater than that of Otsu, MCE, and the proposed methods. The *MER* values obtained by the proposed method are similar to or less than that of Otsu and MCE method on all test images. In this respect, the proposed method is an effective thresholding method for image segmentation.

In many circumstances, image processing tasks need high real-time performance. For this reason, the computing time of each method on segmentation of above four images is also lists here, and they are shown in Table 6.

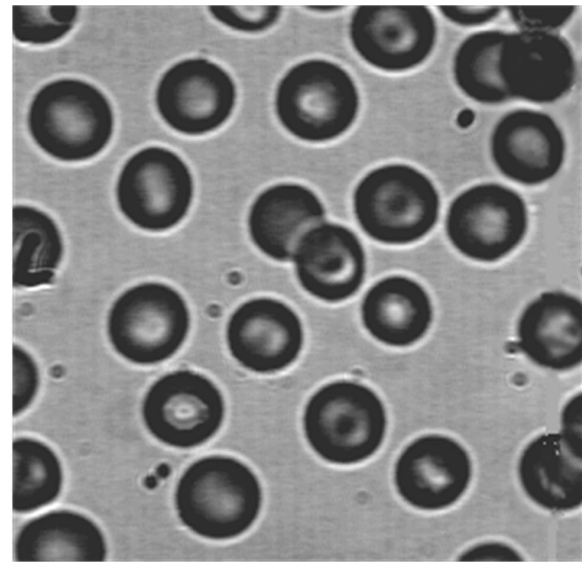
As can be seen from Table 6, the time performance of the proposed method is much better than that of Otsu method. The time consumption of Otsu method is about 5 times that of the proposed method. From Table 6, we also can see that, the time performance of the proposed method is slightly inferior to MCE method, while better than other methods. For the image ‘Img4’ with size of 227×551 , the computing time of the proposed method does not exceed 0.02 seconds. Therefore, from the perspective of time performance, the proposed method meets the needs of real-time task scenarios.

B. Experiments on Other Images

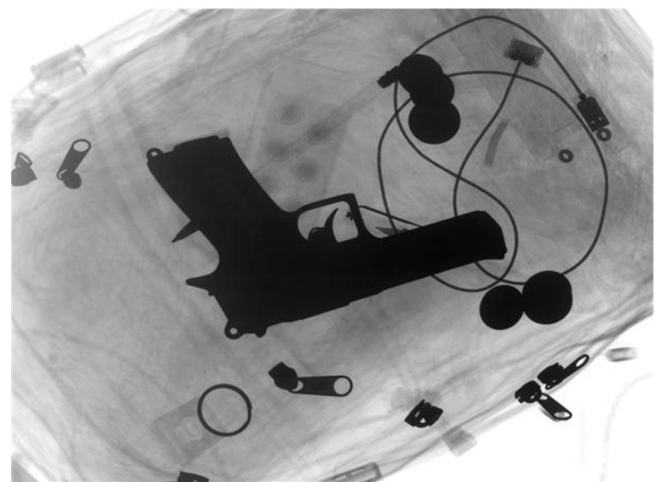
In order to further and better describe the performance of the proposed method, we apply the abovementioned six methods to segmentation of medical image and security check scenario image. Here we choose a medical blood cell image and an X-ray image [23] of security check scenario. The two images are shown in Figure 9. These two images are called ‘blood1’ image and ‘X-ray’ image here. The sizes of these two images are 265×272 and 452×612 , respectively.

Figure 10 shows the grayscale histograms of the ‘blood1’ image and the ‘X-ray’ image. It can be seen from Figure 10 that the distribution of the gray level histogram of the ‘blood1’ image is very sparse, and the gray level histogram of the ‘X-ray’ image is irregularly distributed with multiple peaks.

Table 7 lists the optimal thresholds and computing time of 6 methods on the segmentation of these two images.



(a) blood1 image



(b) X-ray image

Fig. 9. A medical image and an X-ray image for testing

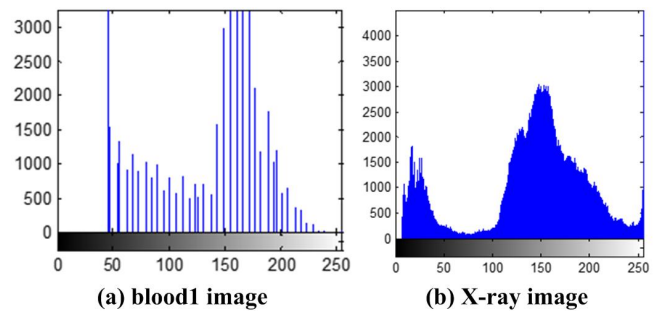


Fig. 10. The histograms of blood1 image and X-ray image

Figures 11-12 show the segmented results of ‘blood1’ image and ‘X-ray’ image with the six methods.

Figure 11 shows the segmentation results of each method on ‘blood1’ image. It can be seen from Figure 11 that the segmentation results of MET method and Lin method are not good for ‘blood1’ image. The MET method is a bit over-segmented, but the Lin method is a bit under-segmented. The results obtained by other methods are significantly better than those obtained by MET method and Lin method. Relatively speaking, the segmentation result of the proposed method

TABLE VII
THE OPTIMAL THRESHOLDS AND TIME-CONSUMING (SECOND) FOR TWO IMAGES

Method	blood1 image		X-ray image	
	threshold	time	threshold	time
Otsu method	106	0.0749	101	0.2819
MET method	46	0.0113	254	0.0159
MCE method	96	0.0125	78	0.0167
Lin method	176	0.0098	196	0.0171
Cai method	118	0.0156	111	0.0204
Proposed method	101	0.0139	84	0.0184

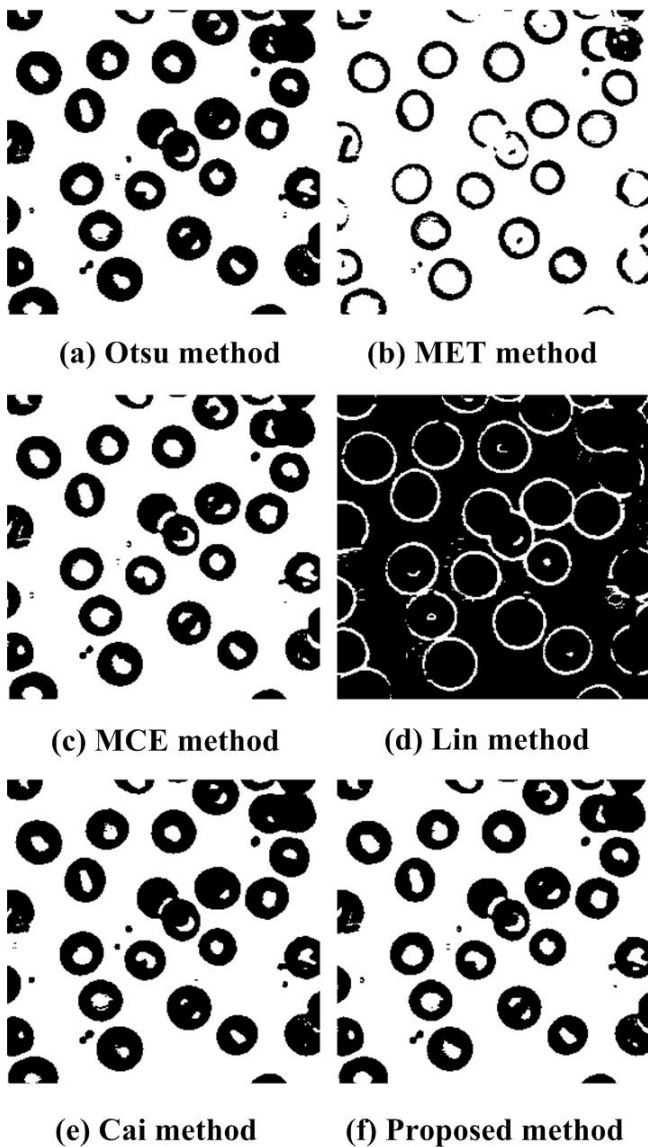


Fig. 11. The threshold segmentation results of blood1 image

is smoother, with fewer residual noise pixels and higher resolution between blood cells.

Figure 12 shows the segmentation results of ‘X-ray’ images for each method. It can be seen from Figure 12 that, it is a complete failure of MET method and Lin method on segmentation of ‘X-ray’ image. For other four methods, the objects that need attention in image are separated from background well. Visually, the results obtained by MCE method and the proposed method are cleaner, and the details

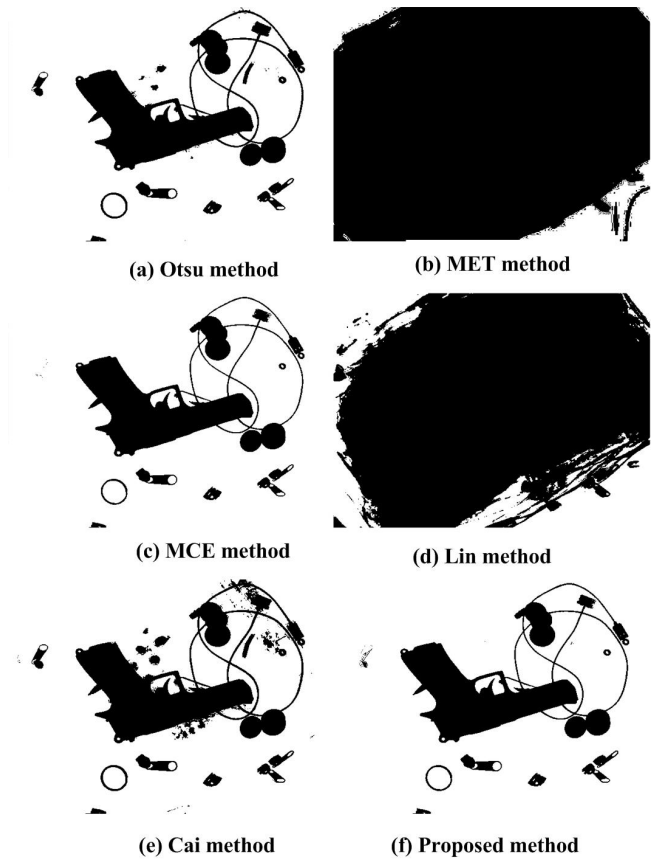


Fig. 12. The threshold segmentation results of X-ray image

of the target are well distinguished.

IV. CONCLUSION

Image segmentation is an eternal topic in the field of image processing. In many scenarios, the existing image segmentation methods are not all effective. It may be necessary to design new methods or transform the old methods to meet the needs of new tasks. Relative arithmetic-geometric divergence is a tool used to measure the similarity (or dissimilarity) between different information systems. Based on the idea of relative arithmetic-geometric divergence, this paper designs and implements a new thresholding method for image segmentation. The new method is applied to the segmentation of non-destructive testing images, degraded document images, medical images and security inspection surveillance images. In the comparison with some classical image threshold segmentation algorithms, the effectiveness of the proposed method is verified. From the experiments, it can be concluded that the proposed method is easy to implement, takes less computation time, and has good segmentation performance, so it has good application and promotion value. At present, this method is only applied to the segmentation of grayscale images. In our future work, the proposed method will be extended to the field of color image segmentation and multi-level image segmentation.

REFERENCES

[1] Pablo Mesejo, Óscar Ibáñez, Óscar Cordon, and Stefano Cagnoni, “A survey on image segmentation using metaheuristic-based deformable models: state of the art and critical analysis,” *Applied Soft Computing*, vol. 44, pp.1-29, 2016.

- [2] Yuanbin Wang, Qian Han, Yuanyuan Li, and Yujie Li, "Video smoke detection based on multi-feature fusion and modified random forest," *Engineering Letters*, vol. 29, no.3, pp.1115-1122, 2021.
- [3] Ahmad Yahya Dawod, Aniwat Phaphuangwittayakul, Fangli Ying, and Salita Angkurawaranon, "Adaptive slices in brain haemorrhage segmentation based on the SLIC algorithm," *Engineering Letters*, vol. 29, no.2, pp.795-802, 2021.
- [4] Albertus Joko Santoso, and Pranowo, "Medical image segmentation using phase-field method based on GPU parallel programming," *Engineering Letters*, vol. 30, no.1, pp.214-220, 2022.
- [5] J.N. Kapur, P.K. Sahoo, and A.K.C. Wong, "A new method for gray-level picture thresholding using the entropy of the histogram," *Computer Vision, Graphics, and Image Processing*, vol. 29, no. 3, pp.273-285, 1985.
- [6] Pankaj Upadhyay, and Jitender Kumar Chhabra, "Kapur's entropy based optimal multilevel image segmentation using Crow Search Algorithm," *Applied Soft Computing*, vol. 97, pp.105522, 2020.
- [7] Dong Zhao, Lei Liu, Fanhua Yu, Ali Asghar Heidari, Mingjing Wang, Guoxi Liang, Khan Muhammad, and Huiling Cheng, "Chaotic random spare ant colony optimization for multi-threshold image segmentation of 2D Kapur entropy," *Knowledge-Based Systems*, pp.106510, 2021.
- [8] C.H. Li, and C.K. Lee, "Minimum cross entropy thresholding," *Pattern Recognition*, vol. 26, no. 4, pp.617-625, 1993.
- [9] C.H. Li, and P.K.S. Tam, "An iterative algorithm for minimum cross entropy thresholding," *Pattern Recognition Letters*, vol. 19, no. 8, pp.771-776, 1998.
- [10] P.D. Sathya, R. Kalyani, and V.P. Sakthivel, "Color image segmentation using Kapur, Otsu and Minimum Cross Entropy functions based on Exchange Market Algorithm," *Expert Systems with Applications*, vol. 172, pp.114636, 2021.
- [11] Bo Lei, and Jiulun Fan, "Multilevel minimum cross entropy thresholding: A comparative study," *Applied Soft Computing*, vol. 96, pp.106588, 2020.
- [12] Bo Wu, Jianxin Zhou, Xiaoyuan Ji, Yajun Yin, and Xu Shen, "An ameliorated teaching-learning-based optimization algorithm based study of image segmentation for multilevel thresholding using Kapur's entropy and Otsu's between class variance," *Information Sciences*, vol. 533, pp.72-107, 2020.
- [13] J. Kittler, and J. Illingworth, "Minimum error thresholding," *Pattern Recognition*, vol. 19, no. 1, pp.41-47, 1986.
- [14] Fujiki Morii, "A note on minimum error thresholding," *Pattern Recognition Letters*, vol. 12, no. 6, pp.349-351, 1991.
- [15] Fan Jiulun, and Xie Winxin, "Minimum error thresholding: A note," *Pattern Recognition Letters*, vol. 18, no. 8, pp.705-709, 1997.
- [16] Jiulun Fan, "Notes on Poisson distribution-based minimum error thresholding," *Pattern Recognition Letters*, vol. 19, no. 5-6, pp.425-431, 1998.
- [17] Inder Jeet Taneja, "Relative divergence measures and information inequalities," *Inequality Theory and Applications*, vol. 5, pp.145-168, 2005.
- [18] M. Sezgin, B. Sankur, "Survey over image thresholding techniques and quantitative performance evaluation," *Journal of Electronic Imaging*, vol. 13, no. 1, pp.146-165, 2004.
- [19] Hongmin Cai, Zhong Yang, Xinhua Cao, Weiming Xia, and Xiaoyin Xu, "A new iterative triclass thresholding technique in image segmentation," *IEEE Transactions on Image Processing*, vol. 23, no. 3, pp.1038-1046, 2014.
- [20] N. Otsu, "A threshold selection method from gray-level histograms," *IEEE Transactions on Systems, Man, and Cybernetics*, vol. 9, no.1, pp.62-66, 1979.
- [21] Qianqian Lin, and Congjie Ou, "Tsallis entropy and the long-range correlation in image thresholding," *Signal Processing*, vol. 92, pp.2931-2939, 2012.
- [22] Kishore Dutta, Dhritiman Talukdar, and Siddhartha S. Bora, "Segmentation of unhealthy leaves in cruciferous crops for early disease detection using vegetative indices and Otsu thresholding of aerial images," *Measurement*, vol. 189, pp.110478, 2022.
- [23] Domingo Mery, Vladimir Riffo, Uwe Zscherpel, German Mondragón, Iván Lillo, Irene Zuccar, Hans Lobel, and Miguel Carrasco, "GDxray: The database of X-ray images for nondestructive testing," *Journal of Nondestructive Evaluation*, vol. 34, pp.42, 2015.